



Computation of Nanowire Transport Properties

Bahaaudin M. Raffah^{1,2} and Paul C. Abbott^{1,*}

¹School of Physics, M013, The University of Western Australia, 35 Stirling Highway, Crawley, WA 6009, Australia

²Faculty of Science, Physics Department, King Abdulaziz University, P. O. Box 80203, Jeddah, Saudi Arabia

With the rapid increase in the development and modelling of nanodevices, efficient, accurate, and general computation of transport properties is required. This paper presents the *Mathematica* package **TransportCoefficients**, which uses the *R*-matrix method to compute the transmission and reflection coefficients for an arbitrary potentials in one dimension, and for two dimensions in cylindrical coordinates.

Keywords: Wigner-Eisenbud Functions, Computer Algebra, Hybrid Symbolic-Numeric Computation, *R*-Matrix Methods, Quantum Transport, Cylindrical Nanowires.

1. INTRODUCTION

In recent years, research has led to the development of complex nanowires which appear promising for the implementation of quantum circuits.^{1–3} For example, in 2008, the Samsung company fabricated a nanowire with a gate length of 15 nm and a radius of 4 nm, where the gate is wrapped around a metal wire.⁴ However, manufacturing nanowires is expensive and time-consuming so modelling them is the logical approach before application in the laboratory or industry.^{5–7} This requires code for evaluating transport properties, such as transmission coefficients, quickly and accurately for a wide range of problems, and for arbitrary potentials.

The *R*-matrix method has wide application to transport phenomena.⁸ Evaluating Wigner-Eisenbud Functions (WEFs) and their eigenenergies is the first step of the procedure using the *R*-matrix formalism, as described in Ref. [9]. The second step is to construct the scattering states which contain all the information necessary to calculate the reflection and transmission coefficients.^{10,11} These two steps provide a natural description of all electron transport properties in nanodevices.

This paper presents the *Mathematica* package **TransportCoefficients**, which computes transmission coefficients for one and two dimensions in cylindrical coordinates. Section 2 summarises the theory of the WEFs in two dimensions. Applications of the *R*-matrix formalism to 1D and 2D scattering problems is then demonstrated. Dimensionless units permit application of the Wigner-Eisenbud method to a wide range of physical systems, not restricted to nanoscale quantum devices. In Section 3,

WEFs are computed using the Fourier Discrete Cosine Transform (DCT), followed by 1D and 2D examples. Various potentials are then examined, with visualisations and analysis of the corresponding transmission coefficients.

An alternative quantum dynamical implementation for evaluating the transport properties of cylindrical quantum nanowires is presented in Raffah and Wang.¹²

2. THEORY

2.1. 1D Wigner-Eisenbud Functions

The 1D WEFs, $\chi_l(z)$, arise as solutions to the scaled Schrödinger equation,⁹

$$-\chi_l''(z) + V(z)\chi_l(z) = E_l\chi_l(z) \quad (1)$$

over $[-1, 1]$ with Neumann boundary conditions $\chi_l'(\pm 1) = 0$. To compute $\chi_l(z)$ we write

$$\chi_l(z) = \sum_{p=0}^{\infty} c_p^{(l)} \varphi_p(z) \quad (2)$$

where $\varphi_p(z)$ is the p th orthogonal trigonometric basis function, which corresponds to DCT type 3 (DCT-III) (Fig. 1).

Introducing the potential energy matrix element

$$\langle P | V | p \rangle = \int_{-1}^1 \varphi_p(z)V(z)\varphi_p(z) dz \quad (3)$$

which is computed by applying the DCT to a uniform sampling of the potential,⁹ leads to the following matrix eigenproblem,

$$\left(\frac{\pi p}{2}\right)^2 \delta_{P,p} + \langle P | V | p \rangle = E \langle P | p \rangle \quad (4)$$

from which E_l and $c^{(l)}$, and hence χ_l , are obtained.

*Author to whom correspondence should be addressed.

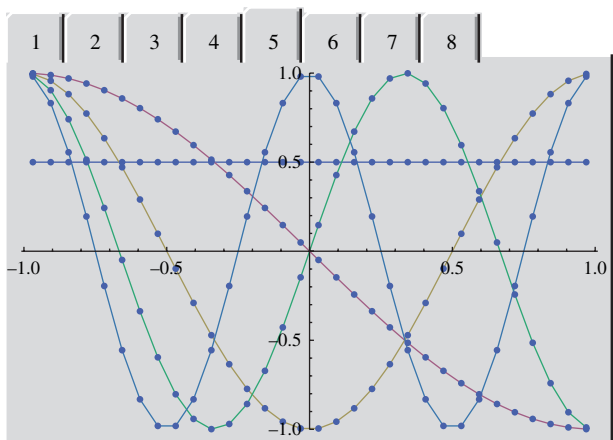


Fig. 1. DCT-III basis.

2.2. 2D Wigner-Eisenbud Functions

In this section, we consider a 2D cylindrical geometry (Fig. 2). The scaled 2D Schrödinger equation in cylindrical coordinates reads^{1,9}

$$\begin{aligned} H\chi_l(r, z) &= (s^2 T_r^{(m)} + T_z + V(r, z))\chi_l(r, z) \\ &= E_l \chi_l(r, z) \end{aligned} \quad (5)$$

where $s = d/R$ is a dimensionless scale factor (see Fig. 2). $T_r^{(m)}$ and T_z are the radial and axial kinetic energy operators,

$$T_r^{(m)} = -\left(\frac{\partial^2}{\partial r^2} + \frac{1}{r} \frac{\partial}{\partial r} - \frac{m^2}{r^2}\right), \quad T_z = -\frac{\partial^2}{\partial z^2} \quad (6)$$

for (r, z) in $[0, 1] \times [-1, 1]$, along with the boundary conditions

$$\chi_l(1, z) = 0, \quad \chi_l^{(0,1)}(r, \pm 1) = 0 \quad (7)$$

Solving Eq. (5) gives the complete set of WEFs representing the wavefunction inside the scattering region.^{1,5,9} Separating variables in Eq. (5), $\chi(r, z) \rightarrow \phi(r)\varphi(z)$, and applying the boundary conditions, leads to a complete basis for constructing the WEFs.

The complete orthonormal set of radial basis functions is expressed in terms of Fourier-Bessel functions.^{13,14} The functions $\{\phi_k^{(m)}(r)\}_{k=1,2,\dots}$ satisfy

$$T_r^{(m)} \phi_k^{(m)}(r) = j_{m,k}^2 \phi_k^{(m)}(r) \quad (8)$$

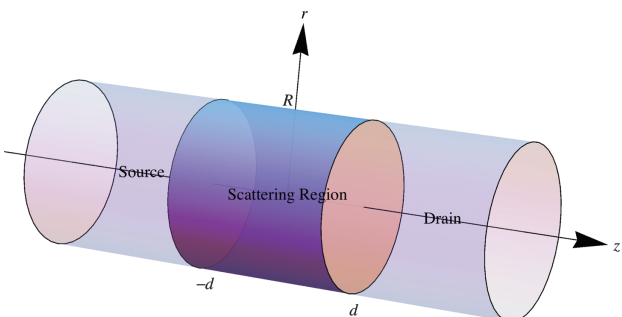


Fig. 2. Geometry for a cylindrical nanowire.

where

$$\phi_k^{(m)}(r) = \frac{\sqrt{2} J_m(j_{m,k} r)}{J_{m+1}(j_{m,k})}, \quad \phi_k^{(m)}(1) = 0 \quad (9)$$

and $j_{m,k}$ is the k th zero of the Bessel function $J_m(x)$.

The general 2D WEF then reads

$$\chi_l(r, z) = \sum_{k=1}^{\infty} \sum_{p=0}^{\infty} c_{k,p,m}^{(l)} \phi_k^{(m)}(r) \varphi_p(z) \quad (10)$$

If the potential satisfies $V(r, z) = V(z)$, which arises in cases of physical interest considered in this paper, orthonormality of the radial basis functions converts Eq. (5) to the matrix eigenproblem,^{1,5,9,10,15}

$$\left(E_{\perp} + \left(\frac{\pi p}{2}\right)^2\right) \langle P | p \rangle + \langle P | V | p \rangle = E \langle P | p \rangle \quad (11)$$

where $E_{\perp} = s^2 j_{m,k}^2$ is the transversal eigenenergy corresponding to the mode $\phi_k^{(m)}(r)$.^{1,5} Appropriate truncation of Eq. (10) is determined by the energy ordering of the Hamiltonian matrix, from which E_l and $c^{(l)}$, and hence χ_l , are obtained following the usual steps.^{1,5,9,10,15}

2.3. R-Matrix Formalism for 1D Scattering Problem

The χ_l are evaluated for the scattering region and then the incident wavefunction from the asymptotic region is matched with them at the scattering boundaries using the *R*-matrix formalism.^{1,10,11,15,16} In 1D, the *R*-matrix is defined as

$$\mathbf{R}(E) = \begin{pmatrix} R(E; -1, -1) & R(E; 1, -1) \\ R(E; -1, 1) & R(E; 1, 1) \end{pmatrix} \quad (12)$$

where the (dimensionless) *R*-function is

$$R(E; z, z') = \frac{\pi}{2} \sum_{l=1}^{\infty} \frac{\chi_l(z)\chi_l(z')}{E - E_l} \quad (13)$$

The scattering matrix $\mathbf{S}(E)$ is calculated directly from $\mathbf{R}(E)$,

$$\mathbf{S}(E) = \mathbb{I} - 2[\mathbb{I} + i\mathbf{R}(E)\mathbf{K}(E)]^{-1} \quad (14)$$

where \mathbb{I} is the unit matrix, and $\mathbf{K}(E)$ is the diagonal wave vector matrix of the incident electron,¹⁵

$$\mathbf{K}(E) = \frac{2}{\pi} \begin{pmatrix} \sqrt{E - V_1} & 0 \\ 0 & \sqrt{E - V_2} \end{pmatrix} \quad (15)$$

which depends upon the values of the potential V_i at the scattering region boundaries, $V_1 = V(-1)$, $V_2 = V(+1)$.

The scattering wave functions $\psi^{(i)}(E, z)$ with $i = 1, 2$ are constructed using the *R*-function and the scattering matrix,

$$\begin{aligned} &\begin{pmatrix} \psi^{(1)}(E, z) \\ \psi^{(2)}(E, z) \end{pmatrix} \\ &= \frac{i}{\sqrt{2\pi}} \Theta(E) [1 - \mathbf{S}(E)^T] \mathbf{K}(E) \begin{pmatrix} R(E; -1, z) \\ R(E; 1, z) \end{pmatrix} \end{aligned} \quad (16)$$

- (3) Use the appropriate (operating-system dependent) commands to move `QuantumDynamics.tgz` into the user's AddOns directory.
- (4) Extract the `QuantumDynamics` folder into the user's AddOns directory.
- (5) In *Mathematica*, load the `TransportCoefficients.m` package by executing the following command:

```
<<QuantumDynamics`TransportCoefficients`
```

- (6) To check that the `TransportCoefficients.m` package has been loaded, along with `WignerEisenbud.m` and `WignerEisenbud2D.m`, and to provide a list of functions defined in the package, execute the following commands:

```
<<QuantumDynamics`TransportCoefficients`*
<<QuantumDynamics`WignerEisenbud`*
<<QuantumDynamics`WignerEisenbud2D`*
```

3.2. Wigner-Eisenbud Functions

In 1D the WEFs, and matrix elements of (uniformly sampled) functions, are computed using the DCT.⁹ The Fourier-Bessel basis (9) is used to compute the radial part of 2D WEFs. This requires computing zeros of the Bessel function $J_m(x)$. To speed up the code, the first 500 zeros of the Bessel function $J_m(x)$ are computed and saved:

```
JZeros /: JZeros[m_] := JZeros /: JZeros[m] = N[BesselJZero[m, Range[500]]]
FourierBesselFunction[m_, k_, r_] :=  $\frac{\sqrt{2} \text{BesselJ}[m, \text{JZeros}[m][[k]]]r}{\text{BesselJ}[m+1, \text{JZeros}[m][[k]]]}$ 
```

For potentials that are independent of r , $V(r, z) = V(z)$, the 2D Wigner-Eisenbud function $\chi(r, z)$ is separable. Define the transversal energy E_{\perp} :

```
TransversalEnergy[m_, k_, s_]:=s^2 JZeros[m][[k]]^2
```

Next, appropriate truncation of Eq. (11) is determined. The general function `OrderedPairs` returns the first n indexed elements of the sorted list obtained by applying f to pairs of elements taken from two lists:

```
OrderedPairs[list1_List, list2_List,
n_Integer?Positive, f_:Plus]:=Take[
Sort[
Flatten[
MapIndexed[Flatten[{##}]&,
Outer[f, Sort[list1],
```

```
Sort[list2]], {2}], 1
], n
]
```

`kp[{m, s}, v]` gives the lowest-order Wigner-Eisenbud energies, indexed by k and p :

```
kp[{m_, s_, v_List}]:= kp[{m, s}, v] = OrderedPairs [s^2 JZeros[m]^2, WignerEisenbudEnergies[v], 3 Length[JZeros[m]]]
```

`TotalEnergy[{l_, m_, s_}, v_List]` returns the Wigner-Eisenbud energy with index l :

```
TotalEnergy[{l_, m_, s_}, v_List] := kp[{m, s}, v][[l, 1]]
```

Supplementary code has been developed to allow users to input arbitrary axial potentials.⁹ Realistic potentials are asymmetrical and irregular. Figures 3 and 4 display the 1D and 2D WEFs for a semiconductor heterostructure potential with several layers.^{17,18}

3.3. 1D R-Matrix Formalism

This section presents an application of 1D WEFs to nanodiodes, computing the scattering wavefunctions, transport coefficients, and resonance energies.

The *R*-matrix, $\mathbf{R}(E)$, is defined via the dyadic product of normalised WEFs, computed for the given scattering potential and evaluated at the edge of the scattering region, $\chi_l(\pm 1)\chi_L(\pm 1)$. The following code implements Eq. (12), returning a function dependent upon the incident energy:

```
R[V_List]:=R[V]=Module[{epsilon=WignerEisenbudEnergies[V], chi=WignerEisenbudFunctions[V]}, epsilon Evaluate[ $\frac{\pi}{2} \frac{1}{\epsilon - \epsilon_0} ((v \mapsto v \otimes v) / @ \chi[[All, {1, -1}]])]$ ]
```

Define the scattering matrix (14), $\mathbf{S}(E)$, and diagonal wave vector matrix (15), $\mathbf{K}(E)$:

```
I=IdentityMatrix[2];
S[V_List][epsilon_?NumericQ]:=I-2 Inverse[I+V[V][epsilon].K[V][epsilon]];
K[V_List][epsilon_]:= $\frac{2}{\pi} \begin{pmatrix} \sqrt{\epsilon - V[[1]]} & 0 \\ 0 & \sqrt{\epsilon - V[[2]]} \end{pmatrix}$ 
```

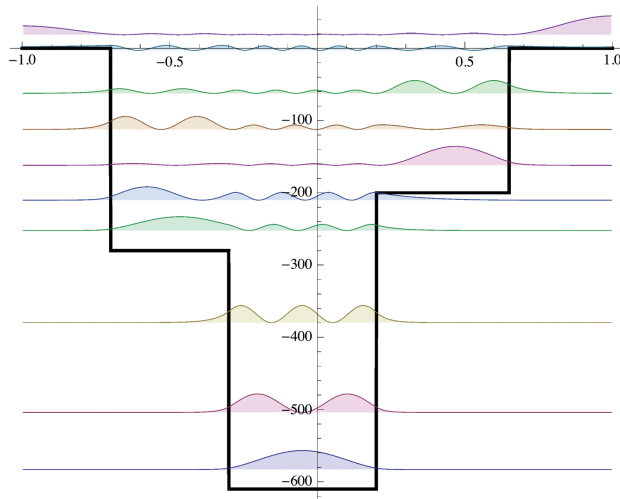


Fig. 3. Lowest order 1D WEFs, $|\chi_l|^2$, shifted upwards by E_l for an irregular potential $V(z)$.

Define the current scattering matrix (18):

$$\begin{aligned} \tilde{\mathbf{s}}[\mathcal{V}_{\text{List}}][\mathcal{E}_{\text{?NumericQ}}] \\ := \text{MatrixPower}[\mathcal{K}[\mathcal{V}][\mathcal{E}], 1/2].\mathcal{S}[\mathcal{V}][\mathcal{E}] \\ \cdot \text{MatrixPower}[\mathcal{K}[\mathcal{V}][\mathcal{E}], -1/2] \end{aligned}$$

A simple example that shows resonance phenomena is scattering from a double potential well. Figure 5(a) shows the WEFs computed using the DCT for a sloping double-step potential well. In Figure 5(b) the scattering wavefunctions are drawn at vertical positions determined by their corresponding resonance energies E_{0l} , which are close to the Wigner-Eisenbud energies E_l . Figure 5(c) displays the position of the first five poles in the complex energy plane, $E_{0l} - i\Gamma_l/2$ (*cf.* [15, Fig. 4.2]). In Figure 6, the position and half-width of the resonance pole corresponding to the $l = 6$ WEF is displayed.

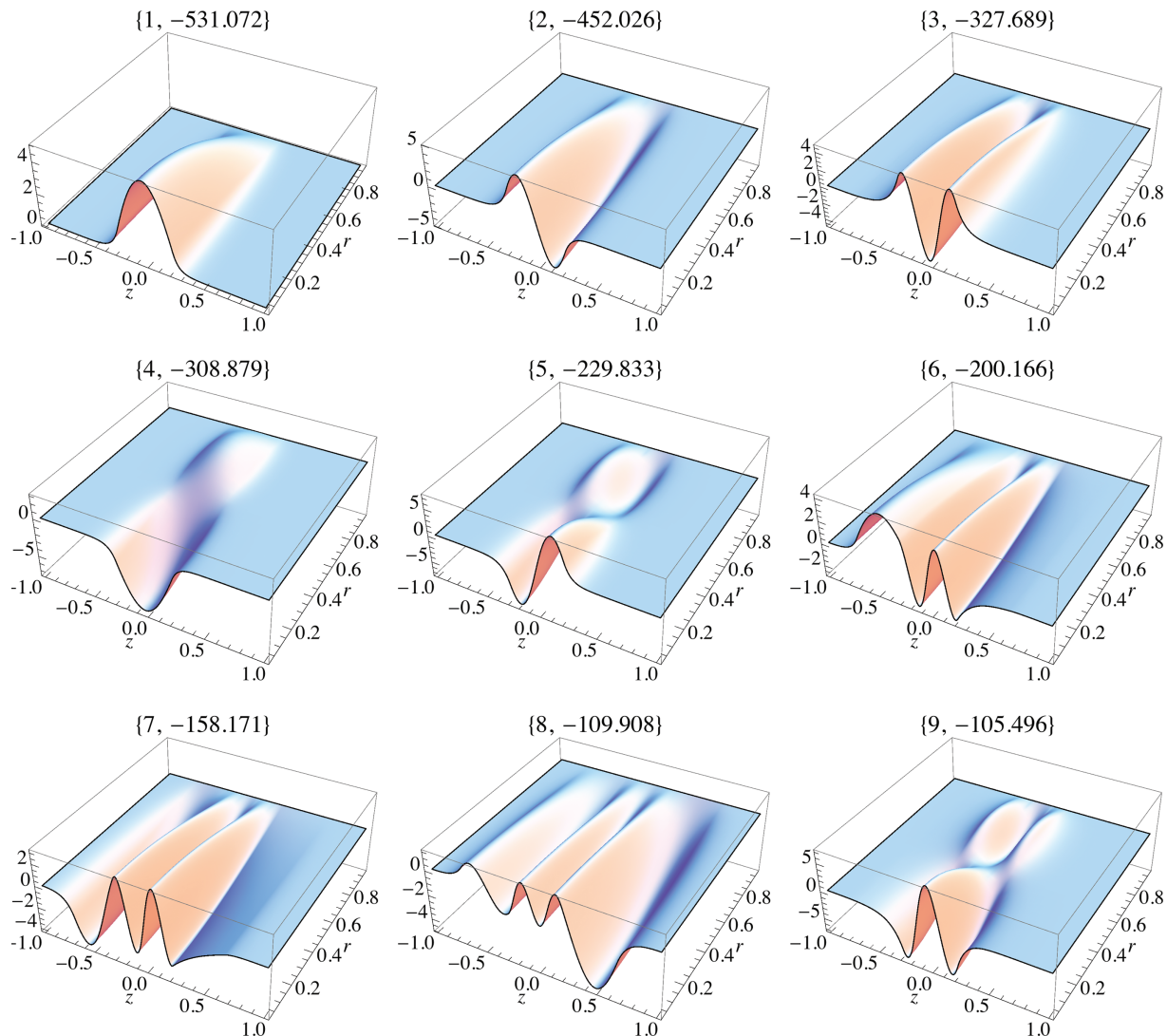


Fig. 4. Lowest-order 2D WEFs, $\chi_l(r, z)$, plotted over $[0, 1] \times [-1, 1]$ and labelled by $\{l, E_l\}$, for the axial potential heterostructure $V(z)$ in Figure 3, with scale factor $s = 3$ and magnetic quantum number $m = 0$.

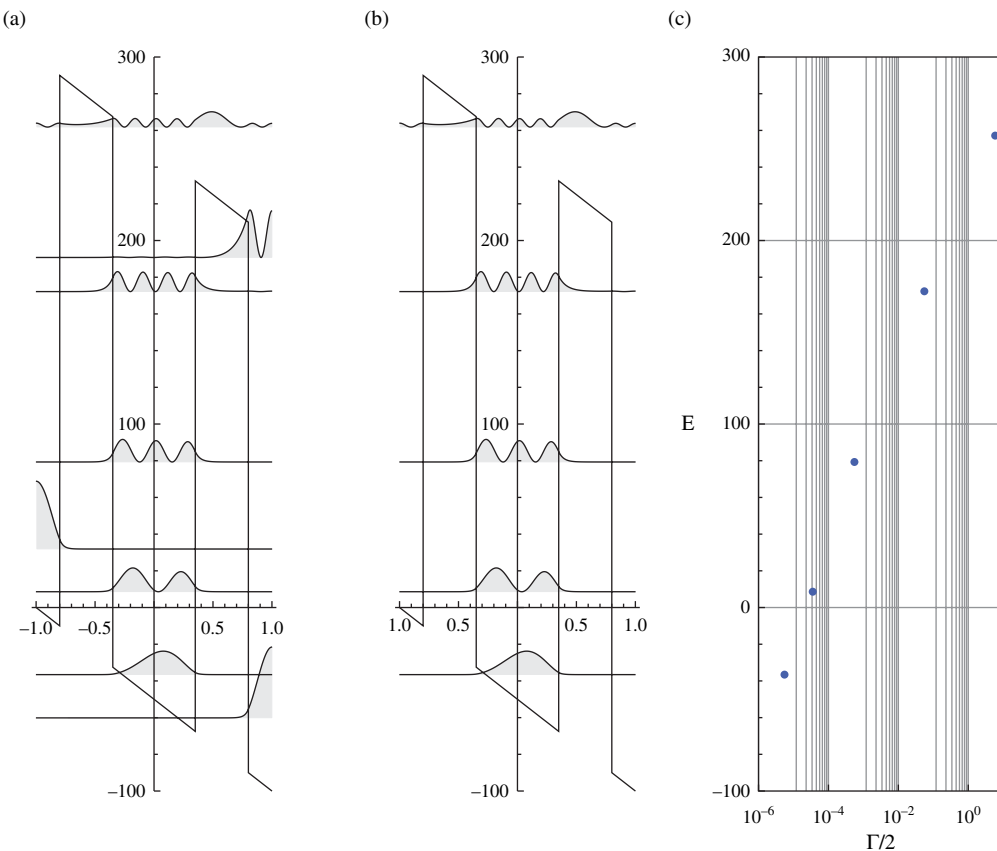


Fig. 5. (a) Low-level WEFs shifted upwards by their eigenvalues E_l for a sloping double-step potential well. (b) Five lowest level scattering wavefunctions shifted upwards by their resonance energies. A scaling factor of 5 has been applied to the wavefunctions in (a) and (b). (c) Plot of resonance poles with energies in dimensionless units.

Implementing Eqs. (22) and (23) for the evaluated current scattering matrix provides the transmission and reflection coefficients, which are displayed in Figure 7. It is verified that these transport coefficients satisfy flux conservation.

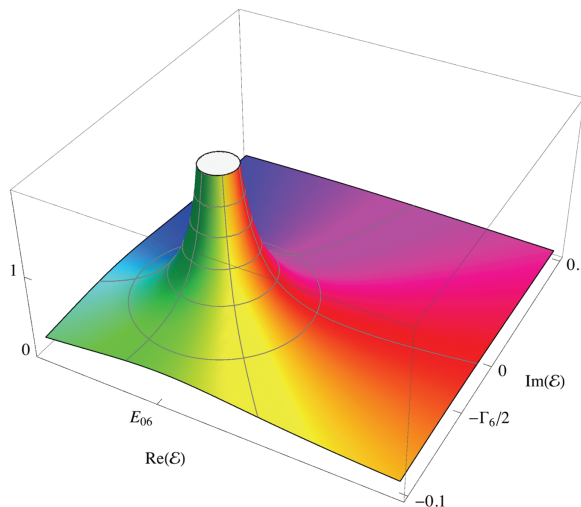


Fig. 6. Plot of $|\tilde{S}(E)|$, phase-coloured by $\arg(\tilde{S}(E))$, over the complex energy plane in the neighbourhood of the resonance pole at $E_{06} - i\Gamma_6/2 \approx 172.334 - 0.04i$.

3.4. 2D R-Matrix Formalism

This section presents an application of the WEFs in two dimensions to evaluate the transmission coefficients in nanodiodes.

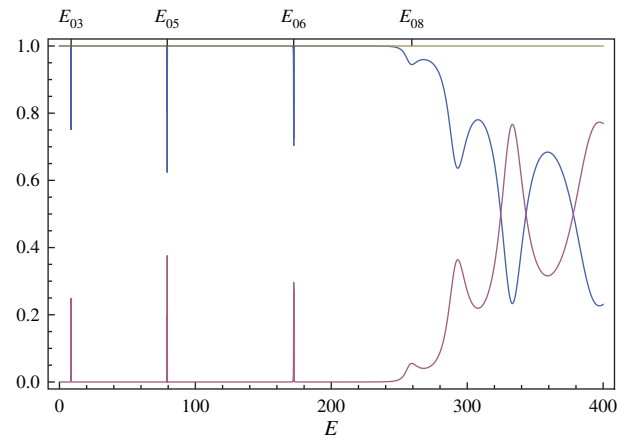


Fig. 7. Plot of the transmission coefficients (red line), $T(E)$, reflection coefficients (blue line), $R(E)$, and flux conservation (yellow line), $T(E) + R(E) = 1$, for the potential in Figure 5.

3.4.1. The R Matrix

The size of the **R**-matrix is determined by the maximum k value:

```
kMax[{m_, s_}, v_List]:=Max[kp[{m, s}, v][[All, 2]]]
```

After computing the dyadic product of the normalised Wigner-Eisenbud vectors at $z = \pm 1$, the function **RBlock** places 2×2 dyadic blocks scaled by $\pi/(2(E - E_l))$ in the appropriate location of a sparse array:

```
dyadic[v_List, p_]:=dyadic[v, p]
  =WignerEisenbudFunctions[v][[p, {1, -1}]]
  ⊗WignerEisenbudFunctions[v][[p, {1, -1}]]
RBlock[{m_, s_}, v_][energy_][{e_, k_, p_}]
:=SparseArray[{{k, k} → π 1 / (energy - e)}, {kMax[{m, s}, v], kMax[{m, s}, v]}]⊗dyadic[v, p]
```

Finally, **RMatrix** is constructed using sparse array operations by mapping **RBlock** over the energy-ordered Wigner-Eisenbud states:

```
RMatrix[{m_, s_}, v_List]:=RMatrix[{m, s}, v]=Function[energy,
  Evaluate[Total[RBlock[{m, s}, v]
    [energy] /@ kp[{m, s}, v]]]
```

3.4.2. Current Scattering Matrix

The **K**-matrix is given by Eq. (28) (we choose $V_i = 0$ for the examples of this paper):

```
KMatrix[{m_, s_, n_}]:=KMatrix[{m, s, n}]
=Function[energy, SparseArray[{{k_, k_}
  :> 2/πSqrt[energy - Transversal
  Energy[m, k, s]], {n, n}}]⊗IdentityMatrix[2]
 ]
```

Entries in the unit-step matrix are non-zero only for conducting channels, which requires computing the largest *real* value of k in Eq. (29) for given s , m , and energy E :

```
StepMatrix/:StepMatrix[{m_, s_, n_}]
:=StepMatrix/:StepMatrix[{m, s, n}]
=Function[energy, SparseArray[{{k_, k_}>1/;
  Length[Cases[Thread[s^2JZeros[m]^2 < energy],
  True]]>=k}, {n, n}]⊗IdentityMatrix[2]
 ]
```

The Ω -matrix (20) code is built from the **R**-matrix code:

```
OmegaMatrix[{m_, s_}, v_List][energy_]
:=Module[{k = kMax[{m, s}, v], K12},
  K12 = MatrixPower[KMatrix[{m, s, k}]
[energy], 0.5]; K12.RMatrix[{m, s}, v][energy].K12
 ]
```

Finally, the current scattering matrix (31) is constructed:

```
CurrentScatteringMatrix[{m_, s_}, v_List]
[energy_]:=Module[{k = kMax[{m, s}, v],
  Θ, Id, Ω},
  Θ = StepMatrix[{m, s, k}][energy];
  Id = IdentityMatrix[2k];
  Ω = OmegaMatrix[{m, s}, v]
[energy]; Θ.(Id - 2Inverse[Id + IΩ]).Θ
 ]
```

3.4.3. Reflection and Transmission Probabilities

Equations (32) and (33) are used to compute the transmission and reflection probabilities:

```
TransmissionProbability[{m_, s_}, v_List]
[energy_]:=Total[Abs[Diagonal
```

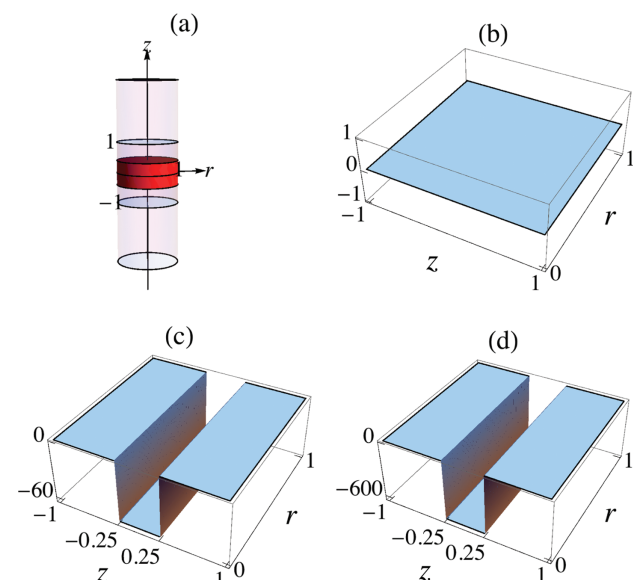


Fig. 8. (a) Quantum dot embedded into a nanowire in dimensionless units. For an effective electron mass of $\mu = 0.19m_e$ with $d = 16$ nm and $s = 3.2$, $1\text{eV} = 1277$ dimensionless energy units. Potential depth equivalent to: (b) $V_b = 0$ eV, (c) $V_c = -0.05$ eV, and (d) $V_d = -0.5$ eV.

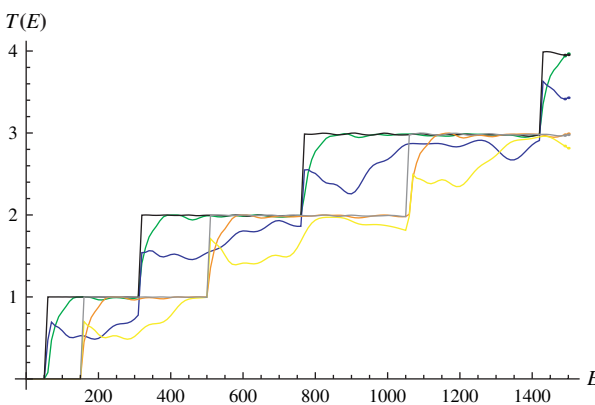


Fig. 9. Plot of total transmission as function of dimensionless energy for the quantum dot potential in Figure 8. The black and gray lines are for $V_b = 0$ eV with $m = 0$ and $m = 1$, respectively; The blue and yellow lines are for $V_c = -0.05$ eV with $m = 0$ and $m = 1$, respectively. The green and orange lines are for $V_d = -0.5$ eV with $m = 0$ and $m = 1$, respectively.

```
[CurrentScatteringMatrix[{m,s},v]
[energy],1]]^2]

ReflectionProbability[{m_,s_},v_List]
[energy_]:=Total[Abs[Diagonal
[CurrentScatteringMatrix[{m,s},v]
[energy]]]^2]/2
```

Delivered by Publishing Technology
IP: 216.185.156.28 On: Thu, 04 Apr 2013
Copyright: American Society of
Engineering Education

3.4.4. Applications

This code was tested on the rectangular quantum well considered by Racec et al. [1, Figures 3 and 4]. Figure 8 displays the potential of a quantum dot embedded into a nanowire, and Figure 9 displays the total transmission coefficients.

4. CONCLUSIONS

We present efficient code for accurate computation of transport coefficients for arbitrary potentials in one dimension, and for two dimensions in cylindrical coordinates. The theoretical and computational details are given for the transmission and reflection coefficients in one and two dimensions, and we demonstrate computation in

both cases. Work is in progress on comparing the electrical characteristics of nanowires using quantum dynamics methods with the results presented here.¹²

Acknowledgments: BR would like to acknowledge support of the King Abdulaziz University and thanks Dr. André B. Fletcher (UWA, School of Physics) for comments on a draft of this paper.

References

- P. N. Racec, E. R. Racec, and H. Neidhardt, *Phys. Rev. B* 79, 155305 (2009).
- S. Tsukamoto, Y. Egami, and T. Ono, *J. Comput. Theor. Nanosci.* 6, 2521 (2009).
- Y. Guo, Y. Kong, W. Guo, and H. Guo, *J. Comput. Theor. Nanosci.* 1, 93 (2004).
- K. H. Cho, K. H. Yeo, Y. Y. Yeoh, S. D. Suk, M. Li, J. M. Lee, M. S. Kim, D. W. Kim, D. Park, B. H. Hong, Y. C. Jung, and S. W. Hwang, *Appl. Phys. Lett.* 92, 052102 (2008).
- H. Neidhardt and P. N. Racec, Modeling of Quantum Transport in Nanowires, ISSN 1437, Berlin (2008).
- T. Ono, Y. Fujimoto, and S. Tsukamoto, *Quantum Matter* 1, 4 (2012).
- Y. Fu, L. Zhang, J. He, C. Ma, L. Chen, and Y. Xu, *J. Comput. Theor. Nanosci.* 7, 528 (2010).
- M. Büttiker, Y. Imry, R. Landauer, and S. Pinhas, *Phys. Rev. B* 31, 6207 (1985).
- B. M. Raffah and P. C. Abbott, *Computer Physics Communications* (2013), (in press), DOI:10.1016/j.cpc.2012.12.027.
- P. N. Racec, Transport Phenomena and Capacitance of Open Quantum Semiconductor Nanostructures, Ph.D. Thesis, Brandenburgische Technische Universität (2002), <http://deposit.ddb.de/cgi-bin/dokserv?idn=965463613>.
- P. N. Racec, E. R. Racec, and H. Neidhardt, R-Matrix Formalism for Electron Scattering in Two Dimensions, Weierstraß-Institut für Angewandte Analysis und Stochastik (2009), ISSN 0946-8633.
- B. M. Raffah and J. B. Wang (2013), manuscript in preparation
- Digital Library of Mathematical Functions. Release 1.0.5, 2012-10-01, <http://dlmf.nist.gov/10.23#P6>.
- R. K. Jain and S. R. K. Iyengar, Advanced Engineering Mathematics, Narosa Publishing House (2002).
- E. R. Racec, Electrons and Optical Phonons in Mesoscopic Semiconductor Heterostructures, Ph.D Thesis, Brandenburgische Technische Universität (2002), <http://deposit.ddb.de/cgi-bin/dokserv?idn=965466566>.
- Y. V. Fyodorov and H. J. Sommers, *J. Math. Phys.* 38, 1918 (1997).
- C. Buizert, F. H. L. Koppens, M. Pioro-Ladrière, H. Tranitz, I. T. Vink, S. Tarucha, W. Wegscheider, and L. M. K. Vandersypen, *Phys. Rev. Lett.* 101, 226603 (2008).
- J. D. Cressler, Silicon Heterostructure Devices, Taylor & Francis Group, LLC (2008).

Received: 17 October 2012. Accepted: 13 November 2012.